RF Breakdown analysis in microstrip structures

F. J. Pérez Soler[(1)] F. Quesada[(2)] M. Mattes[(3)] J. M. Montero[(4)] D. Raboso[(5)]
T. Pinheiro-Ortega[(1)] S. Anza[(1)] C. Vicente[(1)] B. Gimeno[(6)] V. Boria[(7)] J. Gil[(1)]
A. Álvarez[(2)] J. R. Mosig[(3)]

(1) Aurora Software and Testing S. L., Spain
(2) Universidad Politecnica de Cartagena, Spain
(3) Laboratoire d'Electromagnetisme et Acoustique, EPFL-STI-IEL-LEMA
(4) RYMSA Espacio
(5) ESA/ESTEC, The Netherlands
(6) Universitat de Valencia Estudi General
(7) Universidad Politécnica de Valencia

ABSTRACT

In this paper, the outcomes of the currently running ESTEC project No. AO-5086: *New investigations of RF Breakdown in Microwave Transmission Lines* are presented. The objective of the project is to develop a software tool capable to predict the Multipactor and Corona breakdown onsets in shielded microstrip devices, paying special attention to elements like connectors, bridges or ribbons. In the first step, the electromagnetic fields of the devices are computed using an efficient implementation of a Volume/ Surface Integral Equation technique. Secondly, the high power breakdown onsets are determined, employing accurate and realistic models for the electron trajectories and the Secondary Electron Emissions. Also, The Corona Discharge breakdown level is computed by means of the numerical solution of the free electron density continuity equation. Experimental and numerical results are presented, showing good agreement.

1 INTRODUCTION

The investigation in the Multipactor and Corona discharges has been an interesting issue during the last years [1, 2, 3], due to the non-desired effects produced by these kind of phenomena inside electronic devices. In particular, microstrip structures such as filters used in Space Commnunications Systems have been found to be sensitive to such discharges, as they have to be exposed to high power operation levels in vacuum conditions.

The aim of the work is to develop a Sotware Tool which allows obtaining the electromagnetic response of shielded microstrip devices, including the possibility of computing the electric and magnetic fields at any point of the structure. In order to avoid high-density volume segmentations needed in techniques such as Finite Element Methods (FEM), an Integral Equation (IE) approach has been chosen for the electromagnetic analysis. Using a mixed Volume/Surface Integral Equation (VSIE) formulation [4], dielectric substrates can be taken into account as well as the conducting elements. By choosing this approach, only the metallic surfaces and the substrate parts need to be discretized, avoiding the need of meshing the whole air volume which surrounds the shielded device, and leading therefore to smaller numbers of unknowns as compared with other methods. The formulation chosen for the presented tool employs the well-known free space Green's functions, in order to properly deal with these kind of irregularities despite the need to discretize as well the metallic walls that shield the devices. This option has been justified by means of an efficient implementation of the IE, decomposing the Green's function in two parts. First, a static term, which is indepedent on the frequency and contains the singularity of the functions, is evaluated once for the whole geometry. Secondly, a less-singular dynamic term is computed for every frequency point, employing small computational effort. The computational cost is therefore reduced with respect of a standard implementation of the VSIE. This way, the tool is able to provide the electromagnetic response, including the equivalent current densities inside the device and the scattering

parameters, fast and accurately. Once the currents have been obtained, they can be used to compute the electromagnetic fields for any desired point inside the structure.

When the electromagnetic fields at any desired point are obtained, the tool can perform Multipactor and Corona analysis.

For Multipactor simulation, the 3D trajectories of individual free electrons are determined employing the leap-frog integrator, where the value of the fields at each electron location is simply interpolated from the previously calculated grid [5]. When the electrons impact with the boundaries of the miscrostrip structure, either the metallic strip, the substrate or the surrounding box, secondary electrons are emitted according to Vaughan's law [6]. Resonance and electron avalanche are automatically tested for several different input RF powers, determining the multipactor breakdown level.

In order to determine the corona discharge threshold, the free electron density originated by ionisation of the gas molecules inside the waveguide structure has to be computed. To do this, the continuity equation for the evolution of the electron density must be solved [3].

2 ELECTROMAGNETIC THEORY

The Volume/Surface Integral Equation (VSIE) formulation [4] principle is shown in Fig. 1. The formulation considers a general electromagnetic problem composed by a mixture of conducting surfaces and dielectric volumes excited by external sources $\vec{E}^{(exc)}$, as illustrated in Fig. 1(a). By using the well-known surface and volume equivalent principles, the situation can be described as another problem in which the objects are replaced by equivalent surface density currents for the conducting objects and polarization electric currents for the dielectric volumes, which are radiating in the free space (see Fig. 1(b)).

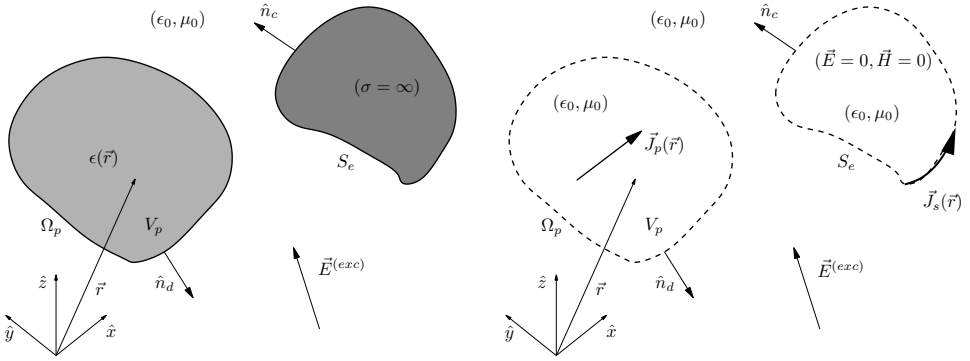

(a) Original problem composed by a dielectric and a conducting body.

(b) Equivalent problem, in terms of electric polarization and surface density currents $\vec{J}_p(\vec{r})$ and $\vec{J}_s(\vec{r})$, each one substituting the dielectric volume and the conducting surface, respectively.

Figure 1: Generic electromagnetic scattering problem and the equivalent situation resulting from the application of the equivalence principles of volumes and surfaces.

Following the procedure in [4], a coupled system of Integral Equations can be obtained as follows:

$$\vec{E}_t^{(exc)}(\vec{r}) = \left\{ -\int_{V_p} \overline{\overline{G}}_{E_J}(\vec{r},\vec{r}\,') \cdot \vec{J}_p(\vec{r}\,')\ dV' - \int_{S_e} \overline{\overline{G}}_{E_J}(\vec{r},\vec{r}\,') \cdot \vec{J}_s(\vec{r}\,')\ dS' \right\}_{S_e} \tag{1a}$$

$$0 = \left\{ \frac{\vec{J}_p(\vec{r})}{j\,\omega\,(\epsilon(\vec{r}) - \epsilon_0)} - \int_{V_p} \overline{\overline{G}}_{E_J}(\vec{r},\vec{r}\,') \cdot \vec{J}_p(\vec{r}\,')\ dV' - \int_{S_e} \overline{\overline{G}}_{E_J}(\vec{r},\vec{r}\,') \cdot \vec{J}_s(\vec{r}\,')\ dS' \right\}_{V_p} \tag{1b}$$

In which $\overline{\overline{G}}_{E_J}$ is the electric field Green's function. However, the authors have preferred to use a mixed potential formulation [7], in order to reduce the singularities that appear in the integrals. The details of this formulation and the application of the Method of Moments (MoM) can be found in [8]. This formulation expresses the IE in terms of the dyadic magnetic vector

potential $\overline{\overline{G}}_A$ and the electric scalar potential G_V, commonly defined as:

$$\overline{\overline{G}}_A = \frac{\mu_0}{4\pi} G \overline{\overline{I}} \tag{2}$$

$$G_V = \frac{1}{4\pi\epsilon_0} G \tag{3}$$

$$G = \frac{e^{-jkR}}{R} \tag{4}$$

For the proposed technique, the general exponential term G of the free space Green's functions can be decomposed as follows:

$$G = \frac{e^{-jkR} - 1}{R} + \frac{1}{R} = G_{dynamic} + G_{static} \tag{5}$$

Applying the decomposition (5), it is possible to decompose the whole MoM matrix of the problem into two parts, corresponding to the dynamic and static parts of the Green's functions. There are two main advantages inherent to the use of this strategy. In first place, the static terms, which are proportional to $(1/R)$, do not depend on the frequency, and can be evaluated once for a given bandwidth of analysis. Secondly, the singular behaviour of the funcions is isolated inside these static terms, reducing the computational effort of the calculation of the remaining dynamic part, which must be evaluated for every frequency. Besides, once the singularity has been extracted from the original function inside the static terms, it can be treated using different techniques. As an important difference with respect to the work [8], where a transformation algorithm from rectangular to cylindrical coordinates is employed, in the proposed tool we have opted for an analytic evaluation to efficiently evaluate the singular integrals, considering rectangular domains in two and three dimensions. These singular integrals have the following expressions:

$$I_1 = \int_S \int_{S'} \frac{1}{R_S}\, dS' dS = -\int_C \int_{C'} R_S\, \vec{u}\vec{u}'\, dl' dl \tag{6}$$

$$I_2 = \int_S \vec{f_t} \int_{S'} \frac{1}{R_S} \vec{f_b}\, dS' dS = -\int_C \int_{C'} R_S\, \vec{u} \cdot \left[\vec{f_t}\vec{f_b} - \vec{f_b}\vec{f_t} + \frac{1}{3}(\vec{f_t}\vec{R}_S - \vec{R}_S\vec{f_b}) + \bar{\bar{I}}(\vec{f_t} \cdot \vec{f_b} - \frac{1}{9} R_S) \right] \cdot \vec{u}'\, dl' dl \tag{7}$$

For metallic surfaces.

$$I_3 = \int_V \int_{V'} \frac{1}{R_V}\, dV' dV = -\frac{1}{2} \int_S \int_{S'} R_V\, \vec{u}\vec{u}'\, dS' dS \tag{8}$$

$$I_4 = \int_V \vec{f_t} \int_{V'} \frac{1}{R_V} \vec{f_b}\, dV' dV = -\frac{1}{2} \int_S \int_{S'} R_V\, \vec{u} \cdot \left[\vec{f_t}\vec{f_b} - \vec{f_b}\vec{f_t} + \frac{1}{4}(\vec{f_t}\vec{R}_V - \vec{R}_V\vec{f_b}) + \bar{\bar{I}}(\vec{f_t} \cdot \vec{f_b} - \frac{1}{12} R_V) \right] \cdot \vec{u}'\, dl' dl \tag{9}$$

In dielectric objects.

$$I_5 = \int_V \int_{S'} \frac{1}{R_V S}\, dS' dV = \frac{1}{2} \left(-\int_0^c \int_S \int_{S'} R_{VS}\, \vec{u}\vec{u}'\, dS' dS dz + \int_S \int_{S'} \frac{c}{R_V|_{(z-z')=c}}\, dS' dS \right) \tag{10}$$

3 RESULTS

In first place, we are interested in some validation results for the electromagnetic tool. Let us consider a simple case of a single microstrip line shielded by a box as shown in Fig. 2(a), where the dimensions are specified. The resulting scattering

parameters are compared in Fig. 2(b) with those obtained by a multilayered spectral method [9], showing a good agreement. The tool is even able to detect the resonant behaviour produced by the metallic shielding of the device around the frequency of 4.7 GHz.

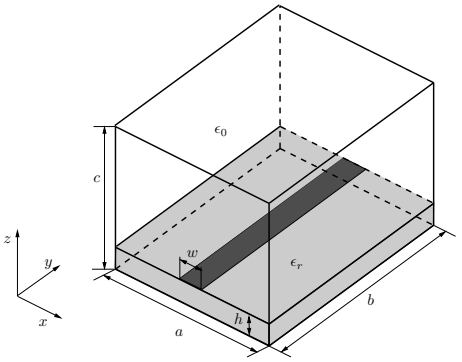

(a) Geometry of the structure. Dimensions are $w = 0.8$mm, $h = 1$mm, $a = b = 40$mm, $c =$4mm. Substrate permittiviy is $\epsilon_r = 9.8$.

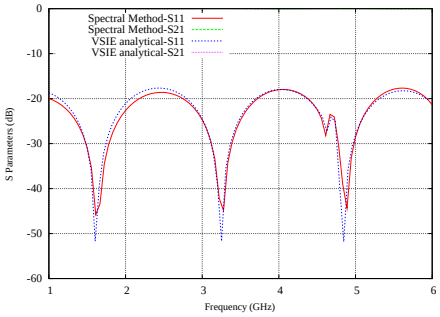

(b) Scattering parameters of the structure. Results of VSIE are compared with a multilayer spectral method [9].

Figure 2: Geometry and scattering parameters of a shielded microstrip line.

The previous result has been used just as validation, as the multilayered technique of [9] is efficient enough to deal with that kind of simple planar structures. Nevertheless, the possibilities of the tool allow to consider more complex geometries, like the one shown in Fig. 3(a), where two dielectric substrates are separated a distance $s = 1.5$ mm, and the metallic strips are connected by means of a rectangular metallic bridge of heigth $h_{bridge} = 0.8$ mm. Also, two cylindrical metallic pins are considered for modelling the exciting coaxial probes that are used in real implementations of these kind of devices. The substrate discontinuity, as well as the vertical currents that appear in the bridge and the pins, cannot be taken into account in planar approaches like [9]. On the contrary, they can be analyzed with the VSIE formulation implemented in the proposed tool with a similar order of complexity as the previous example shown in Fig. 2. The scatterig parameters of this structure are included in Fig. 3(b), showing also a good agreement as compared to a powerful commercial software like HFSS©. The advantage of our technique is the reduction of computational effort by only meshing the substrates and the metallic surfaces, avoiding the massive meshing of the whole volume used in the FEM software. Besides, in a similar way as the adaptative mesh used in HFSS©, refined meshes are also used in our tool, centering the cell density around the metallic strip and the connections, where the electromagnetic fields are more important.

Apart from the smaller computational cost, the most important feature of the tool is the efficient evaluation of the electromagnetic fields at any point in the structures. It is very important to point out the importance of the analytic expressions derived on this purpose. Fig. 4 shows the E_x component obtained along the strip for the example proposed in Fig. 2(a). The observation plane has been placed at $z = 1.1$ mm, very near the metallic strip. If standard numerical integration is performed in the evaluation of the singular integrals of the fields, important numerical error occur, leading to inaccurate results as can be seen in Fig. 4(a). On the other hand, the analytical expressions derived for the tool can successfully remove these errors, obtaining smoothers and more precise results, as can be observed in Fig. 4(b)

High power analysis has been also performed in several structures. In this paper, we present the multipactor results obtained in a gap between two substrates and the flat strip connecting the two sides (the same structure as in Fig. Fig. 3(a), where the height of the bridge is zero $h_{bridge} = 0.8$). Three different structures have been manufactured, with the same dimensions except the distance between the substrates. This distance has been chosen to be 2, 0.5 and 0.3 mm, in order to analyse the impact of the distance between substrates in the multipactor. breakdown onset. Fig. 5(a) shows the Multipactor breakdown levels for these configurations. The results demonstrate that, indeed, the breakdown level increases when reducing the distance between substrates. This can be explained by taking a look to Fig. Fig. 5(b). As the distance between substrates is reduced, electrons do suffer more impacts in their trip between the bottom and the top metallic walls and, therefore, resonance is lost. Interestingly, the results also shows the prediction from the parallel plate approximation which is very conservative as the gap between substrates is reduced since it does not consider the full 3D geometrical environment.

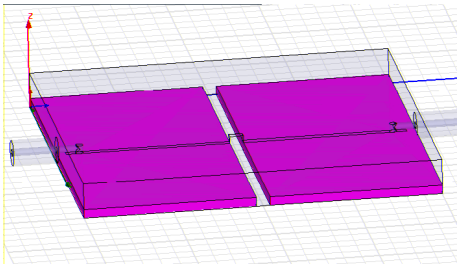

(a) Geometry of the structure. Dimensions are $w = 0.8$mm, $h = 1$mm, $a = b = 40$mm, $c =$4mm. Separation of the substrates is $s = 1.5$mm, and the height of the bridge is $h_{bridge} = 0.8$. Radii, lengths and heights of the two pins are 0.4 mm, 2.5mm and 0.5mm, respectively. Substrate permittiviy is $\epsilon_r = 9.8$.

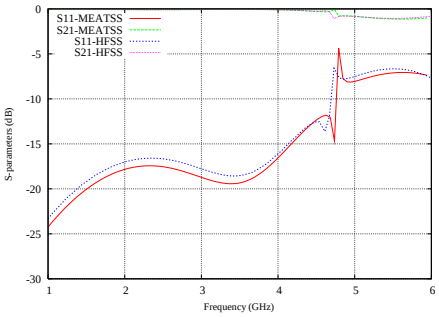

(b) Scattering parameters of the structure. Results of VSIE are compared with Ansoft HFSS© Software.

Figure 3

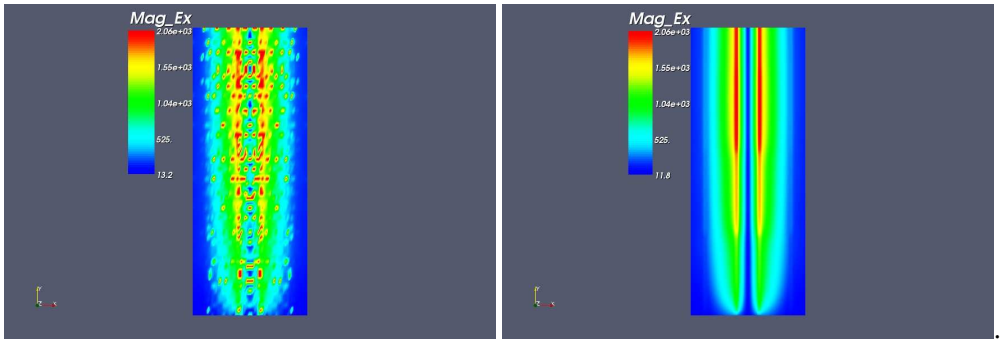

(a) Numerical case (b) Analytical case

Figure 4: Evaluation of the $|E_x|$ field along the strip line using numerical and analytical approaches.

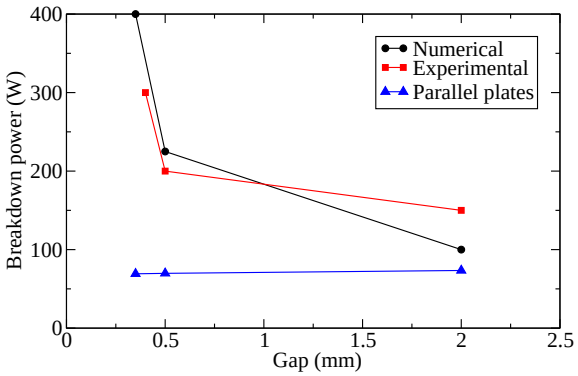

(a) Multipactor breakdown power for different substrate separations.

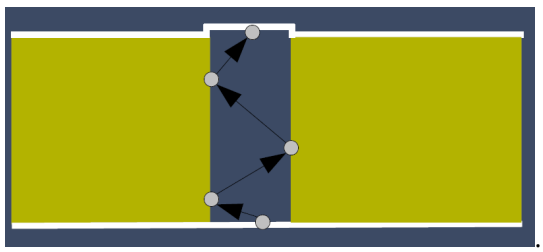

(b) Representation of electron trajectories.

Figure 5: Multipactor breakdown analysis in a bridge zone.

Another example has been chosen to perform corona analysis (see Fig. Fig. 6). In this case, the breakdown occurs around the input connector which pin is connected to the strip by means of a 180 degree ribbon Fig. Fig. 6(b). The electric field is shown together with the comparison between the measurement data and the numerical results.

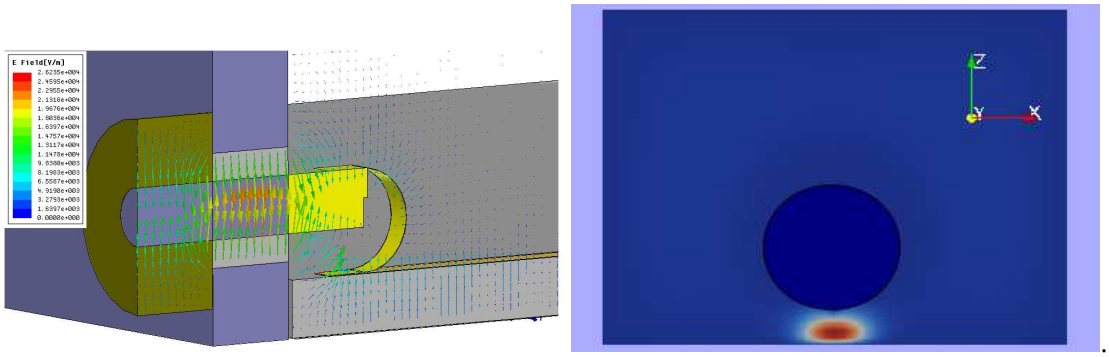

(a) Electric Field around the pin.

(b) Location of the corona discharge.

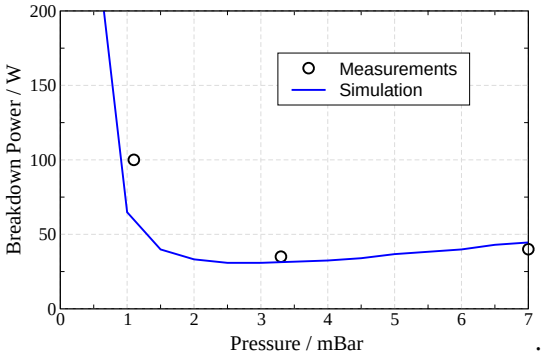

(c) Breakdown power level vs. pressure.

Figure 6: Corona breakdown analysis in a pin zone.

4 CONCLUSIONS

The new software tool has demonstrated its capabilities for the analysis of high power effects on microstip structures. Through the simulation of typical microstrip structures, the VSIE formulation of the field equations has been shown to be accurate and fast when compared to existing commercial simulation tools.

Experimental results have demostrated the need for an accurate software tool capable to handle all aspects regarding the geometry and EM field distribution, in order to predict the RF Breakdown level with accuracy. The tool can be employed to analyse more complicated components involving planar structures.

5 ACKNOWLEDGEMENTS

This work has been supported by the Ministerio de Ciencia e Innovacin of Spain, which has supported this work under the ”Programa Torres Quevedo” (PTQ-08-03-08835).

References

[1] J. Vaughan, “Multipactor,” *IEEE Trans. Electron Devices*, vol. 35, pp. 1172–1180, Jul. 1988.

[2] C. Vicente, M. Mattes, D. Wolk, H. L. Hartnagel, J. R. Mosig, and D. Raboso, “FEST3D: A simulation tool for multipactor prediction,” in *Workshop on Multipactor, RF and DC Corona and Passive Intermodulation in Space RF Hardware*, pp. 11–17, ESTEC, Noordwijk, The Netherlands, Sept. 12-14 2005.

[3] C. Vicente, M. Mattes, D. Wolk, H. L. Hartnagel, J. R. Mosig, and D. Raboso, “FEST3D: A simulation tool for corona prediction,” in *Workshop on Multipactor, RF and DC Corona and Passive Intermodulation in Space RF Hardware*,

pp. 11–17, ESTEC, Noordwijk, The Netherlands, Sept. 12-14 2005.

[4] T. K. Sarkar and E. Arvas, "An integral equation approach to the analysis of finite microstrip antennas: Volume/surface formulation," *IEEE Transactions on Antennas and Propagation*, vol. 38, pp. 305–312, March 1990.

[5] S. Anza, C. Vicente, D. Raboso, J. Gil, B. Gimeno, and V. E. Boria, "Enhanced Prediction of Multipaction Breakdown in Passive Waveguide Components including Space Charge Effects," in *to be published in IEEE International Microwave Symposium Digest*, (Atlanta, USA), June 2008.

[6] J. Vaughan, "A new formula for Secondary Emission Yield," *IEEE Trans. Electron Devices*, vol. 36, pp. 1963–1967, Sept. 1989.

[7] J. R. Mosig, "Arbitrarily shaped microstrip structures and their analysis with a mixed potential integral equation," *IEEE Transactions on Microwave Theory and Techniques*, vol. 36, pp. 314–323, February 1988.

[8] F. Q. Pereira, J. L. G. Tornero, D. C. Rebenaque, J. P. Garcia, and A. A. Melcon, "Analysis of finite microstrip structures using an efficient implementation of the integral equation technique," *Radio Science*, vol. 40, January 2005. doi: 10.1029/2004RS003036.

[9] A. A. Melcon, J. R. Mosig, and M. Guglielmi, "Efficient CAD of boxed microwave circuits based on arbitrary rectangular elements," *IEEE Transactions on Microwave Theory and Techniques*, vol. 47, pp. 1045–1058, July 1999.